A EUROPEAN JOURNAL OF CHEMICAL BIOLOGY

CHEMBIOCHEM

SYNTHETIC BIOLOGY & BIO-NANOTECHNOLOGY

Accepted Article

Title: Effect of Methyl Group on Acyclic Serinol Scaffold for Tethering Dyes on DNA Duplex stability

Authors: Keiji Murayama; Hiroyuki Asanuma

To be cited as: ChemBioChem 10.1002/cbic.201600558

Link to VoR: http://dx.doi.org/10.1002/cbic.201600558

A Journal of

ChemPubSoc Europe

www.chembiochem.org

WILEY-VCH

FULL PAPER WILEY-VCH

Effect of Methyl Group on Acyclic Serinol Scaffold for Tethering Dyes on DNA Duplex stability

Keiji Murayama,[a] and Hiroyuki Asanuma*[a]

Dedication ((optional))

Abstract: Acyclic serinol derivatives are useful scaffolds for tethering dyes within DNA duplexes. Here we synthesized an inverse L-threoninol (iL-threoninol) scaffold and compared its effect on DNA duplex stability to other acyclic artificial nucleic acid scaffolds that are based on D-threoninol, L-threoninol, and serinol. When planar *trans*-azobenzene was incorporated into the DNA duplex through a single bulge-like motif (the wedge), the iL-threoninol scaffold stabilized the duplex most efficiently. When scaffolds were incorporated in complementary positions (dimer motif) or in three adjacent positions (cluster motif), D-threoninol was most stabilizing. Circular dichroism spectra indicated that the effect of scaffold on the duplex stability was closely related to the winding induced by each scaffold. When *trans*-azobenzene was photo-isomerized to non-planar *cis*-azobenzene, iL-threoninol most strongly destabilized duplex irrespective of the number of artificial residues incorporated. The properties of the iL-threoninol scaffold will make it a useful tether for dyes or other functionalities.

Introduction

DNA is an important nanomaterial due to its facile programmability. Although various DNA nanomachines and nanostructures have been constructed, achievable functions are limited when only natural nucleotides A, G, C, and T are used. A large number of chemical modifications on DNA have been reported to provide necessary functions, including artificial nucleobases,[1] phosphate modifications,[2] and substitutions on ribose scaffold.[3] We and others have developed acyclic diol scaffolds that enable incorporation of functional moieties such as dyes into any position of the DNA duplex. In contrast to the natural (deoxy)ribose,[4] acyclic diol scaffolds such as glycerol,[5] serinol,[6] and (*S*)-aminopropane-2,3-diol[7] are readily synthesized and have relatively flexible structures.

Our group has also employed D-threoninol,[8] one of serinol derivatives, as a scaffold for dyes that are *additionally* inserted to DNA duplex as a bulge that does not disrupt adjacent base pairs (Scheme 1a). We have characterized four stable functional motifs that include the D-threoninol scaffold: wedge, dimer, cluster, and interstrand-wedge (Figure 1). Stability results from stacking interactions between the DNA base pairs and, in the case of multiple dye insertions, the dyes themselves. We have also examined the L-threoninol scaffold and shown that it causes severe destabilization of the DNA duplex. This demonstrated that the configuration of 2'-amino group of threoninol is critical (Scheme 1b).[9] Superiority of D-threoninol over L-form allowed us to employ only D-threoninol for introducing functional molecules into DNA.

Aside from above base surrogates, we have also designed three novel acyclic artificial nucleic acids by introducing natural nucleobases into the serinol derivatives: D-*a*TNA[10], L-*a*TNA[11], and SNA[12] from D-threoninol, L-threoninol, and serinol, respectively. When configuration of 2'-amino group is fixed in the same orientation, the only difference among these is position or presence of a methyl group on the main chain of the scaffold (Scheme 1). However, the binding affinities of these artificial oligonucleotides for DNA and RNA were entirely different. D-*a*TNA forms a remarkably stable homo-duplex with complementary D-*a*TNA in an antiparallel manner but does not form stable hybrids with DNA or RNA. In contrast, SNA, which lacks a methyl group, forms stable hybrids with DNA and RNA. Surprisingly, L-*a*TNA, an enantiomer of D-*a*TNA has higher affinity for DNA and RNA than does SNA, indicating the importance of both the methyl group and the configuration of 2'-amino group.

These results prompted us to investigate the methyl group on the acyclic scaffold. In this study, we utilized serinol and *inverse* L-threoninol as a scaffold as well as D-threoninol for tethering functional molecule (Scheme 1d). Scaffolds were functionalized with *trans*-azobenzene and the stabilities of DNA duplexes with three scaffold motifs, the wedge, the dimer, and the cluster, were evaluated.[13] Effect of the methyl group on *trans*-to-*cis* photo-isomerization and on photo-regulatory efficiency were also investigated.

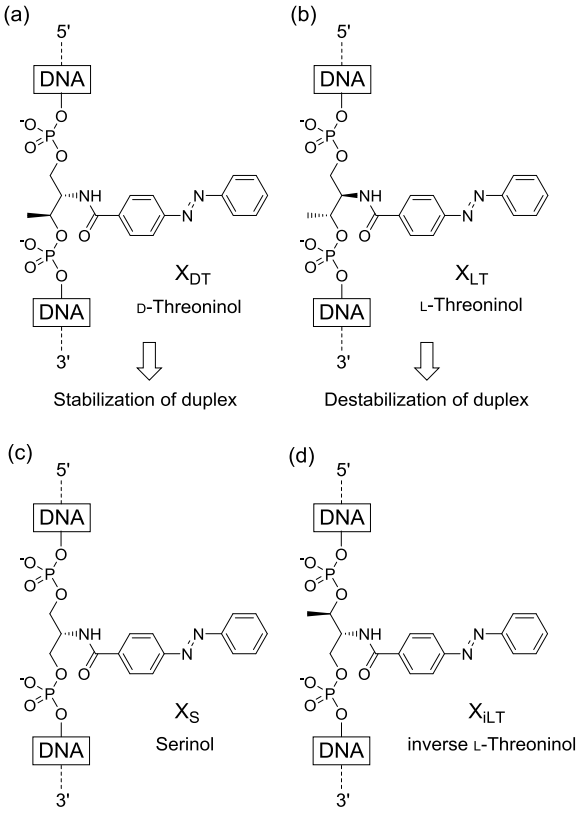

Scheme 1. Structures of acyclic scaffolds carrying azobenzene. Chemical structures of azobenzene incorporated via (a) D-threoninol (X_{DT}), (b) L-threoninol (X_{LT}), (c) serinol (X_S), and (d) inverse L-threoninol (X_{iLT}).

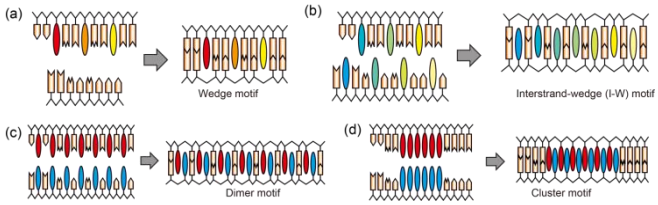

Figure 1. Four functional motifs designed using functionalized acyclic scaffolds incorporated into DNA strands. Ovals represent base surrogates (in this study azobenzene) and interlocking shapes show natural nucleotides.

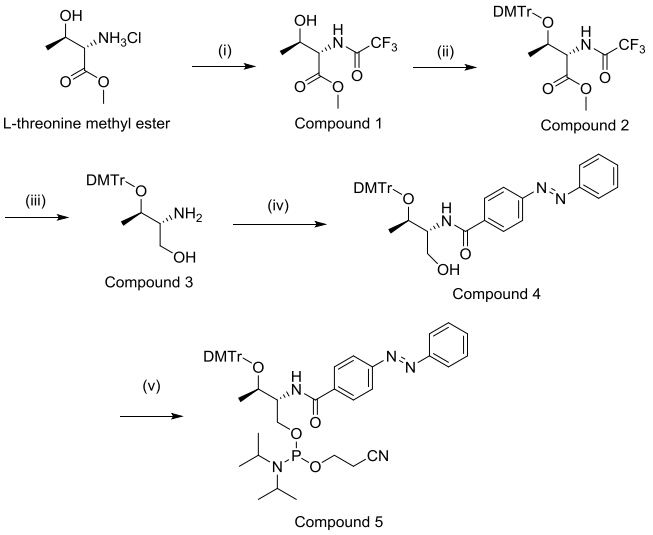

Scheme 2. Synthesis of phosphoramidite iL-threoninol monomer bearing azobenzene: (i) ethyl trifluoroacetate, TEA, MeOH, 0 °C, 30 min, r.t., 1 h, quant.; (ii) 4,4'-dimethoxytrityl (DMTr) chloride, DMAP, DIPEA, pyridine, 65 °C, 12 h; (iii) LiCl, $NaBH_4$, MeOH, THF, 0 °C, 1 h, r.t., 12 h, 21% for 2 steps; (iv) 4-(phenylazo) benzoic acid, 4-(4,6-Dimethoxy-1,3,5-triazin-2-yl)-4-methylmorpholinium Chloride n-Hydrate (DMT-MM), TEA, DMF, r.t., 1 h, 68%; (v) 2-cyanoethyl diisopropylchlorophosphoramidite, TEA, CH_2Cl_2, 0 °C, 20 min, 51%.

Results and discussion

Synthesis of base surrogates from iL-theoninol scaffold

To fix the configuration of the 2'-amino group in the desired L-threoninol configuration, the hydroxyl group at the 1' position of L-threoninol must be connected to 5' terminus of a growing DNA strand. Therefore, we designed the *inverse* L-threoninol (iL-threoninol) scaffold (Scheme 1d). To incorporate the azobenzene via the iL-threoninol scaffold (**X_{iLT}**) into DNA, we synthesized phosphoramidite monomer in which 3'-hydroxyl group of L-threoninol was protected with 4,4'-dimethoxytrityl (DMTr) group (Scheme 2, Figure S1): Commercially available L-threonine methyl ester was first protected with trifluoroacetic acid (compound **1**), followed by reaction with DMTr-Cl. Then the obtained compound **2** was reduced to give DMTr-iL-threoninol (compound **3**). The phosphoramidite monomer tethering azobenzene (compound **5**) was synthesized from DMTr-iL-threoninol as previously described.[11]

Synthesized sequences are listed in Table 1. One (**N-1X**, **C-1X**) or three azobenzenes were incorporated adjacent to each other (**N-3X-c**, **C-3X-c**) or separated by natural nucleotides (**N-3X**, **C-3X**) into native DNA strands (**N**, **C**). Duplexes were prepared by combining these strands with suitable counter strands: wedge motif (**N-1X/C** and **N-3X/C**), single and triple dimer motifs (**N-1X/C-1X** and **N-3X/C-3X**), and the cluster motif (**N-3X-c/C-3X-c**).[8] Additionally, we also prepared a DNA strand containing FAM (**FAM-DNA**) and a complementary sequence tethering DABCYL and nine azobenzenes (**DAB-9X**) to enable fluorescence-based analysis of association and dissociation of the strands as reported previously.[14] Oligonucleotides were

synthesized containing base surrogate prepared from D-threoninol ($\mathbf{X_{DT}}$), serinol ($\mathbf{X_S}$), and iL-threoninol ($\mathbf{X_{iLT}}$).

Table 1. Sequences of synthesized oligonucleotides.

Name	Sequences [a]
N	5'-GGTATCGCAATC-3'
N-1X	5'-GGTATC**X**GCAATC-3'
N-3X	5'-GGT**X**ATC**X**GCA**X**ATC-3'
N-3X-c	5'-GGTATC**XXX**GCAATC-3'
C	3'-CCATAGCGTTAG-5'
C-1X	3'-CCATAG**X**CGTTAG-5'
C-3X	3'-CCA**X**TAG**X**CGT**X**TAG-5'
C-3X-c	3'-CCATAG**XXX**CGTTAG-5'
DAB-9X	5'-CT**X**TT**X**AA**X**GA**X**AG**X**GA**X**GA**X**TA**X**TA**X**CC-**DABCYL**-3' [b]
FAM-DNA	3'-GAAATTCTTCCTCTATATGG-**FAM**-5' [c]

[a] **X** represents azobenzene-tethered monomer (X_S, X_{DT}, or X_{iLT}). [b] 3'-DABCYL-CPG (Glen Research) was used to incorporate DABCYL. [c] FAM was conjugated using 5'-fluorescein phosphoramidite (Glen Research).

Wedge motif

In wedge motif, the base surrogate is a bulge within a natural DNA or RNA duplex. This motif has been used in a stemless linear probe and in photoresponsive DNA duplexes.[15] Thermal stability of duplexes containing $\mathbf{X_{DT}}$, $\mathbf{X_S}$, and $\mathbf{X_{iLT}}$ were evaluated by analysis of thermally induced melting (Figure 2, Figure S2, and Table S1). The melting temperature (T_m) of native **N/C** duplex was 47.7 °C. The duplex containing one *trans*-azobenzene linked via D-threoninol (**N-1X$_{DT}$/C**) had a T_m of 49.2 °C higher than that of the native duplex as we reported before[9]. The T_m of the duplex containing the *trans*-azobenzene linked via iL-threoninol (**N-1X$_{iLT}$/C**) was 50.2 °C, which was higher than that of **N-1X$_{DT}$/C** duplex. The serinol-containing duplex (**N-1X$_S$/C**) had a T_m of 47.7 °C, identical to that of the native **N/C** duplex. The T_m difference was enhanced when three azobenzenes were introduced: the **N-3X$_{iLT}$/C** duplex had a T_m of 55.7 °C and the **N-3X$_{DT}$/C** duplex had a T_m of 53.6 °C. Even the serinol-containing duplex **N-3X$_S$/C** had a higher T_m than the native DNA. Thus, stacking interaction among three planar *trans*-azobenzenes and adjacent base pairs stabilized all duplexes containing acyclic scaffolds relative to the native DNA. The configuration of 2'-amino group was important because the duplex containing the L-threoninol scaffold (Scheme 1b) was significantly less stable than that containing iL-threoninol and D-threoninol.[9] The methyl group on the serinol derivative was also important as further evidenced when nine surrogates were incorporated. The T_m was 60.3 °C for **DAB-9X$_{iLT}$/FAM-DNA**, whereas duplexes with $\mathbf{X_{DT}}$ and $\mathbf{X_S}$ were 4.0 and 5.0 °C lower than this, respectively.

Analyses of van't Hoff plots revealed that the stabilization of **DAB-9X$_{iLT}$/FAM-DNA** relative to duplexes with $\mathbf{X_{DT}}$ and $\mathbf{X_S}$ was attributed to a larger enthalpy change (Table S2), reflecting the more favourable stacking interaction of *trans*-azobenzene when incorporated on iL-threoninol. Hence, duplex stability of wedge motif was in the order of $X_{iLT} > X_{DT} > X_S$. iL-Threoninol is the best scaffold among three for incorporating planar molecule into DNA as wedge motif.

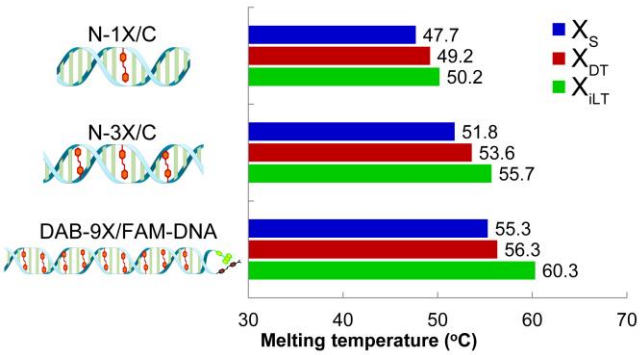

Figure 2. Melting temperatures of duplexes containing azobenzenes in wedge motif. Azobenzene was incorporated as $\mathbf{X_S}$ (blue bars), $\mathbf{X_{DT}}$ (red bars), and $\mathbf{X_{iLT}}$ (green bars). All modified duplexes were stabilized relative to native DNA (**N/C**: T_m = 47.7 °C). Conditions: 5.0 μM DNA, 10 mM phosphate buffer (pH 7), 100 mM NaCl. Azobenzenes were isomerized to *trans*-form by irradiating with 450 nm light at room temperature before measurement.

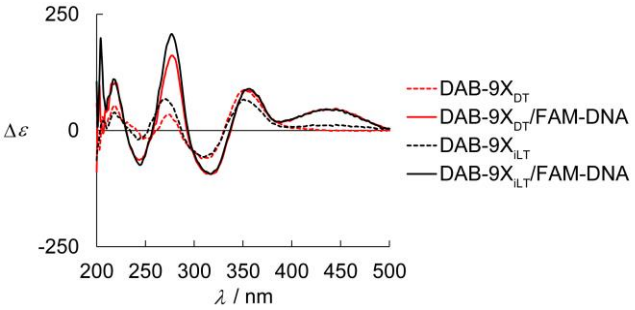

Figure 3. CD spectra of single stranded **DAB-9X** (broken lines) and **DAB-9X/FAM-DNA** duplexes (solid lines) at 20 °C. Red lines are spectra of **DAB-9X$_{DT}$** and black lines are **DAB-9X$_{iLT}$**.

In order to elucidate the effect of methyl group on the scaffold on the duplex structure, we compared CD spectra of duplexes containing nine azobenzenes linked through each scaffold. As shown in Figure 3, in the 300-500 nm region where azobenzene has absorption, the CD spectra of the duplex with D-threoninol (red solid line) almost coincided with that with iL-threoninol (black solid line).[16] On the contrary, the CD intensity at 275 nm was slightly lower for the D-form than for iL-form, indicating the D-form resulted in a slightly unwound duplex relative to the iL-form. Single-stranded **DAB-9X$_{DT}$** (red broken line) also showed smaller CD signal at 270 nm than did single-stranded **DAB-9X$_{iLT}$** (black broken line). Our previous analysis showed that L-*a*TNA

forms a stable duplex with DNA and RNA whereas D-*a*TNA does not.[11] Our data suggest that the right-handed nature of iL-threoninol stabilizes the right-handed DNA duplex, whereas the slight unwinding due to D-threoninol is less stabilizing. However, achiral serinol scaffold destabilized duplex compared with D-threoninol and iL-threoninol. Probably, the methyl group of threoninol also contributes to the stabilization of the duplex, likely through van der Waals interactions with adjacent scaffold residues.

Dimer and cluster motifs

Next, we evaluated thermal stabilities of duplexes with dimer and cluster motifs. Interestingly, dimer motif (**N-1X/C-1X** and **N-3X/C-3X**) showed different tendency from wedge motif. T_m values of duplexes with a single pair of *trans*-azobenzenes were 51.9 °C for **N-1X$_{DT}$/C-1X$_{DT}$**, 50.8 °C for **N-1X$_{iLT}$/ C-1X$_{iLT}$**, and 49.9 °C for **N-1X$_S$/C-1X$_S$** (Figure 4, Figure S2, and Table S1). When three azobenzene pairs were incorporated, D-threoninol remarkably stabilized the duplex (**N-3X$_{DT}$/C-3X$_{DT}$**; T_m = 59.7 °C) compared to the other two scaffolds (**N-3X$_{iLT}$/C-3X$_{iLT}$**; T_m = 56.3 °C, **N-3X$_S$/C-3X$_S$**; T_m = 55.2 °C). Similarly in the cluster motif (**N-3X-c/C-3X-c**), D-threoninol was the most stable duplex, although difference between D- and iL-scaffold was only about 1 °C. Thus, D-threoninol was the most suitable scaffold for clustering the planar molecules within DNA duplexes.[17]

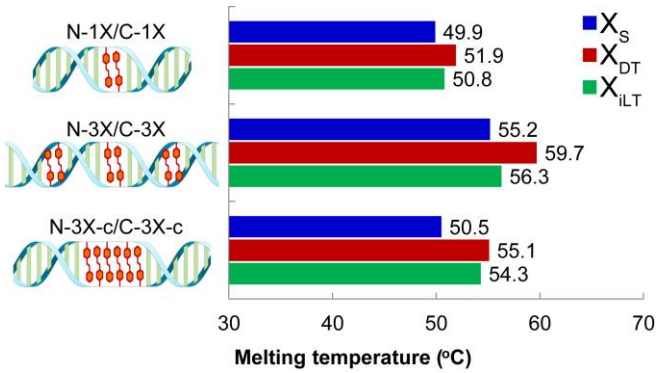

Figure 4. Melting temperatures of duplexes with acyclic scaffolds in dimer and cluster motifs. Azobenzene was incorporated using **X$_S$** (blue bars), **X$_{DT}$** (red bars), and **X$_{iLT}$** (green bars). Solution conditions were 5.0 μM DNA, 100 mM NaCl, 10 mM phosphate buffer (pH 7.0), 20 °C.

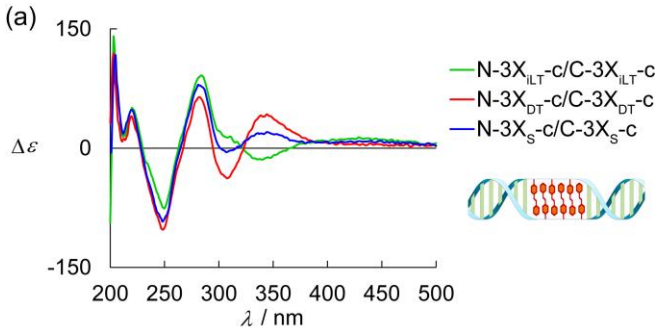

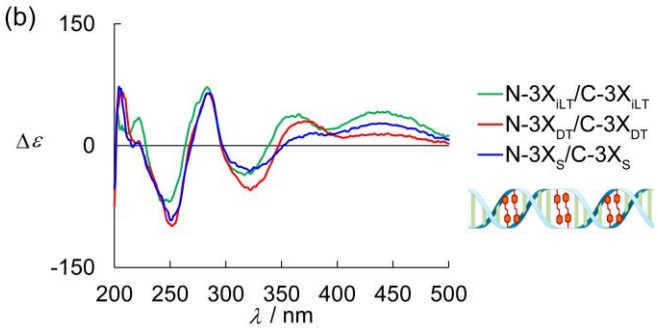

Figure 5. CD spectra of DNA bearing **X$_{iLT}$** (green lines), **X$_{DT}$** (red lines), and **X$_S$** (blue lines) recorded at 20 °C. Spectra of DNA duplexes (a) **N-3X-c/C-3X-c** and (b) **N-3X/C-3X** are shown. Conditions: 4.0 μM DNA, 100 mM NaCl, 10 mM phosphate buffer (pH 7.0), 20 °C.

We then analysed the CD spectra of duplexes that were modified with dimers and clusters of azobenzene. For duplexes modified with the cluster motif, the CD spectra depended on the scaffolds (Figure 5a). The CD spectrum of the D-threoninol-containing cluster motif duplex (**N-3X$_{DT}$-c/C-3X$_{DT}$-c**) was characterized by a positive-to-negative Cotton effect between 300 and 370 nm corresponding to azobenzene absorption, indicative of a right-handed helical structure in the azobenzene region. In contrast, iL-threoninol (**N-3X$_{iLT}$-c/C-3X$_{iLT}$-c**) yielded negative-to-positive Cotton effect in the same region of the spectrum, suggestive of a left-handed helix. This hypothesis is reasonable because the iL-threoninol scaffold is an enantiomer of the D-scaffold. These CDs are interpreted that, unlike wedge motif, D-threoninol induced right-handed helical cluster whereas iL-form did left-handed helix when planar functional molecules were incorporated as interstrand cluster. The higher T_m of **N-3X$_{DT}$-c/C-3X$_{DT}$-c** compared to **N-3X$_{iLT}$-c/C-3X$_{iLT}$-c** may be due to a better fit of the right-handed azobenzene region with the right-handed helical nature of the natural DNA duplex on either side. The duplex modified with the serinol cluster had the lowest T_m, probably due to the lower stability of azobenzene hexamer; as discussed at the wedge motif, methyl group on the main chain itself would stabilize the cluster.

In the duplexes with three pairs of azobenzenes (**N-3X/C-3X**), CD spectra were similar irrespective of the scaffold (Figure 5b). Between 300 and 400 nm, positive-to-negative Cotton effects were observed, indicating that the azobenzene pairs wind clockwise. Dimeric azobenzenes on iL-threoninol would prefer to wind counter clockwise, but the natural base pairs adjacent to the azobenzene likely force the azobenzene dimer to twist in a clockwise manner. The higher T_m of **3X$_{DT}$-c/C-3X$_{DT}$-c** compared to **N-3X$_{iLT}$-c/C-3X$_{iLT}$-c** reflects the coincidence of helical property of D-threoninol.

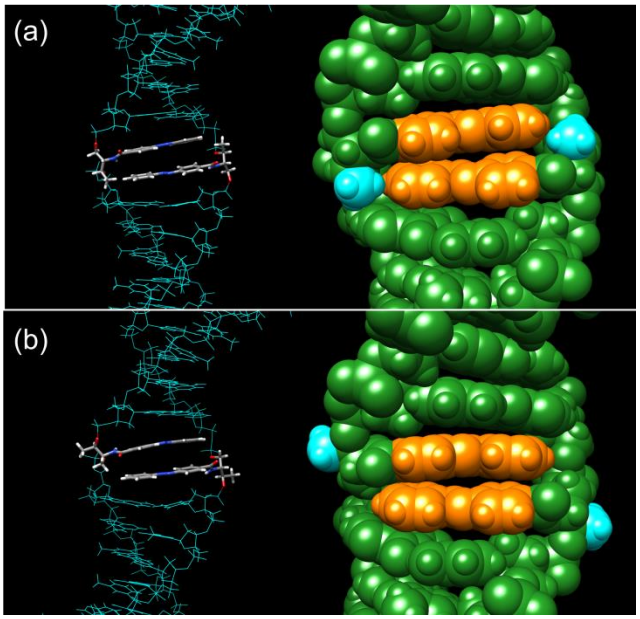

Figure 6. Energy minimized structures of (a) **N-1X$_{DT}$/C-1X$_{DT}$** and (b) **N-1X$_{iLT}$/C-1X$_{iLT}$** duplexes. Left: DNA strands are coloured cyan and the X_{DT} atoms are variously coloured. Right: Structures depicted as CPK models with natural DNA in green, azobenzene in orange, and the scaffold in blue. Azobenzene and the methyl group of D-threoninol scaffold appear to interact.

We also conducted computer-based modelling using the OPLS_2005 force field[18] to obtain energy minimized structures of **N-1X$_{DT}$/C-1X$_{DT}$** and **N-1X$_{iLT}$/C-1X$_{iLT}$** (Figure 6). The azobenzenes on either D- or iL-threoninol scaffolds intercalated without causing distortion of duplex, but the positions of the methyl groups in the duplex were different. The methyl group of the D-threoninol scaffold was located close to the azobenzene moiety in the opposite strand (Figure 6a). A close contact between the methyl group and azobenzene was not observed with the iL-scaffold (Figure 6b). This contact may contribute to the stabilization of dimer motif in the **N-1X$_{DT}$/C-1X$_{DT}$** duplex.

Trans-to-*cis* photo-isomerization in each motif

We have reported that *trans-cis* isomerization of azobenzene linked to DNA via D-threoninol reversibly photo-regulates formation and dissociation of the DNA duplex upon irradiation with UV or visible light.[13] Hence, we determined the T_ms of duplexes in which azobenzene linked via the L-threoninol scaffold was in the *cis* form and evaluated *trans-to-cis* isomerization efficiency. Figure 7a shows the UV-Vis spectra of duplexes with the wedge motif at 20 °C after irradiation with either 360 or 450 nm light. To maximize *cis* isomerization, duplexes were irradiated with 360 nm light at 60 °C, a temperature at which mostly single strands were present. At the photo-stationary state, about 90% of azobenzenes were in the *cis* conformation after irradiating with 360 nm light and about 90% of azobenzenes were in the *trans* conformation after irradiation with 450 nm irrespective of the scaffolds. All duplexes showed essentially no difference on the isomerization ratio among scaffolds (Figure S3).

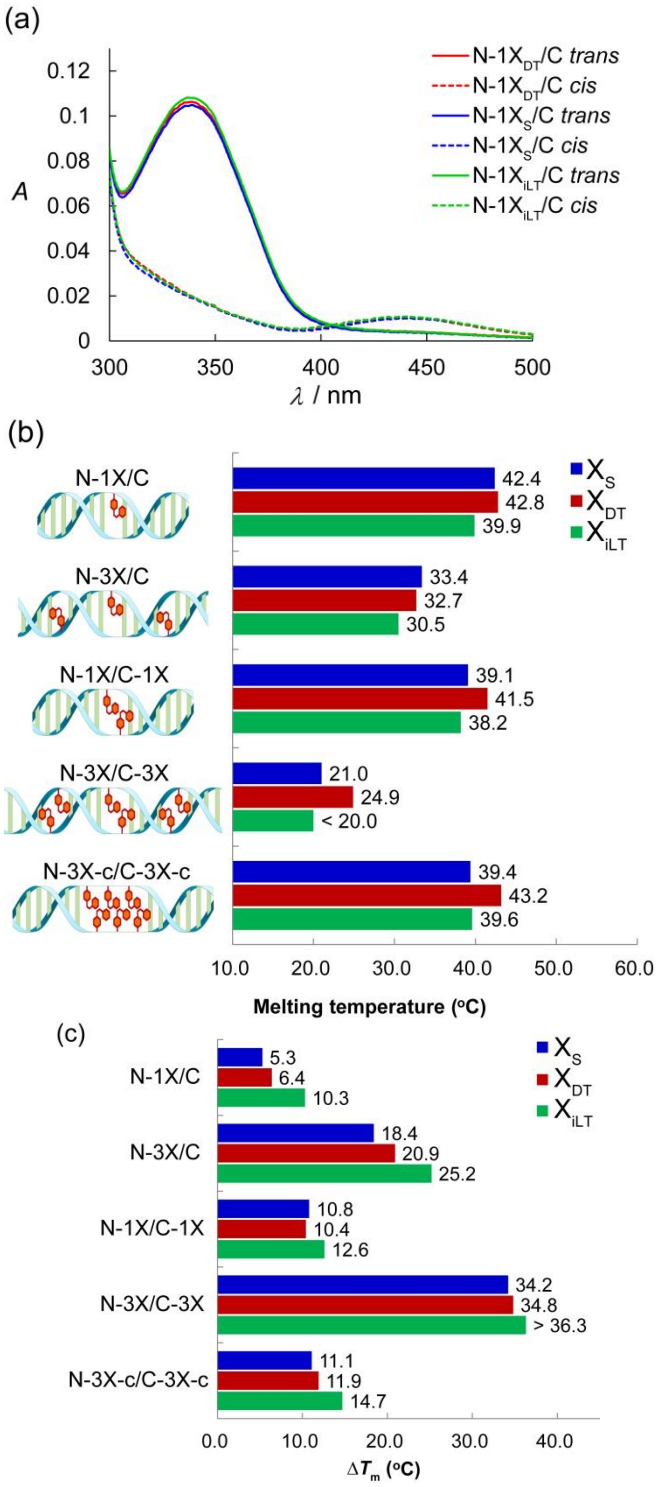

Figure 7. (a) Absorption spectra of **N-1X/C** duplexes after irradiation with at 450 nm at 20 °C (solid lines) or at 360 nm at 60 °C (broken lines). X_{DT} (red lines), X_S (blue lines), and X_{iLT} (green lines) were incorporated into DNA strands. (b) Melting temperatures of duplexes tethering *cis* azobenzenes. Azobenzene was incorporated as **X$_S$** (blue bars), **X$_{DT}$** (red bars), and **X$_{iLT}$** (green bars). Azobenzenes were isomerized to the *cis* form by irradiating with 360 nm light at 60 °C. (c) ΔT_m between *trans*- and *cis*-azobenzene-containing duplexes. Conditions: 5.0 μM DNA, 10 mM phosphate buffer (pH 7.0), 100 mM NaCl.

In the context of the wedge motif, the T_m of the duplex with the *cis* form on iL-threoninol (**N-1X$_{iLT}$/C**; 39.9 °C) was significantly lower than that on D-threoninol (**N-1X$_{DT}$/C**; 42.8 °C) or serinol (**N-1X$_S$/C**; 42.4 °C) as shown in Figure 7b. The difference in melting temperature (ΔT_m) between the duplexes with *trans* and *cis* forms was higher for iL-threoninol (ΔT_m = 10.3 °C) than for duplexes with the other scaffolds (Figure 7c). When three azobenzenes were present (**N-3X/C**) or when the azobenzenes were inserted in the dimer motif (**N-1X/C-1X**), the differences among the scaffolds was enhanced (Figure 7c) with iL-threoninol resulting in maximum ΔT_m values. The destabilization due to *cis* isomerization in cluster motif was smaller than in the other motifs, because this motif can accept even non-planar molecules such as cyclohexane derivatives.[19] Nevertheless, in the cluster motif, the iL-threoninol had the maximum ΔT_m. All these results indicate that iL-threoninol will allow efficient photo-regulation of duplex formation.

Isomerization of azobenzene in duplexes under physiological conditions

Next, we evaluated *trans*-to-*cis* isomerization in the DNA duplexes below the T_m of the duplex containing the *trans* form of azobenzene (20 or 37 °C) where duplex was firmly formed. The change in the absorption spectra of **N-1X$_{iLT}$/C** upon UV-irradiation at 20 °C is shown in Figure 8a, and *cis*-ratios of **N-1X/C** are plotted against the UV-irradiation time in Figure 8b. At 20 °C, about 60-65% azobenzene was isomerized to *cis* form at the photo-stationary state. The efficiency was lower in the duplex as irradiation of the single-stranded **N-1X$_{iLT}$** at 20 °C resulted in over 80% isomerization (Figure 8b). Strong stacking interactions between the *trans* azobenzene and neighbouring base pairs presumably interfere with efficient photo-isomerization as previously described.[14] We did not observe a significant difference in extent of isomerization among scaffolds (Figure 8b).

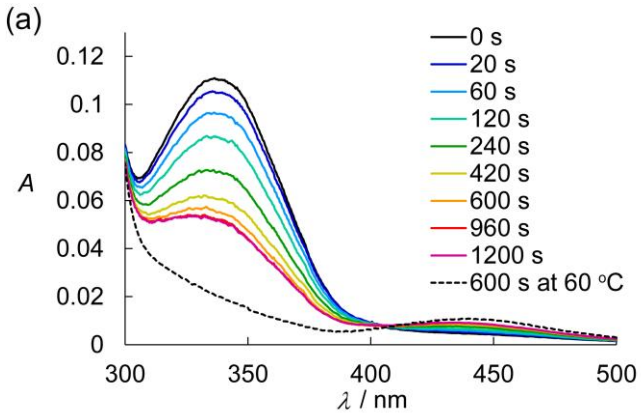

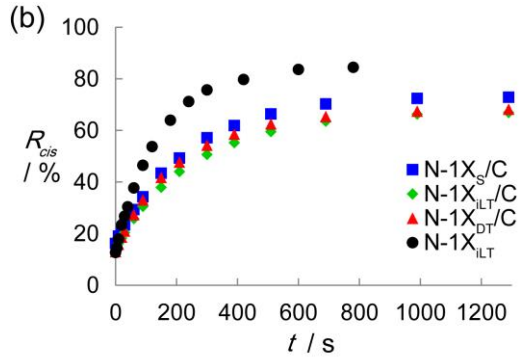

Figure 8. (a) UV-Vis spectra of **N-1X/C** duplexes after indicated times of irradiation at 450 nm at 20 °C. (b) Plots of *cis* ratio vs. time of irradiation with 360 nm light at 60 °C. Solution conditions were 5.0 μM DNA, 100 mM NaCl, 10 mM phosphate buffer (pH 7.0).

Finally, we evaluated photo-regulation of hybridization by analysis of fluorescence of duplexes labelled on one strand with fluorescein (FAM) and on the other with DABCYL. For efficient photo-regulation, nine azobenzenes were incorporated in the wedge motif (**DAB-9X/FAM-DNA**) and the fluorescence change was monitored after irradiation (Figure 9 and S4). Fluorescence from **DAB-9X$_{iLT}$/FAM-DNA** duplex prepared with iL-threoninol was almost completely quenched after irradiation with 450 nm light (Figure 9, red line), indicating duplex formation at 37 °C. In order to maximize *cis* isomerization, the solution was irradiated with UV at 60 °C and cooled to 37 °C prior to evaluation of the spectrum (yellow line). The fluorescence intensity after irradiation and cooling was almost the same as that of single stranded **FAM-DNA** (black line), clearly indicating that complete dissociation results upon *cis* isomerization. When UV irradiation was performed at 37 °C, 88% recovery of the emission was observed (green line). Although 100% dissociation was not attained, very efficient photo-switching was possible under physiological conditions with the **DAB-9X$_{iLT}$/FAM-DNA** duplex. In this sequence context, formation of duplexes with azobenzene linked to D-threoninol and serinol scaffolds was also efficiently controlled by photo-irradiation (Figure S4). Since nine azobenzenes were sufficient for efficient photoregulation, superiority of iL-threoninol may not be reflected to the photoregulatory efficiency.[20] Hence, all three acyclic scaffolds can be used to efficiently photo-regulate nucleic acid hybridization.

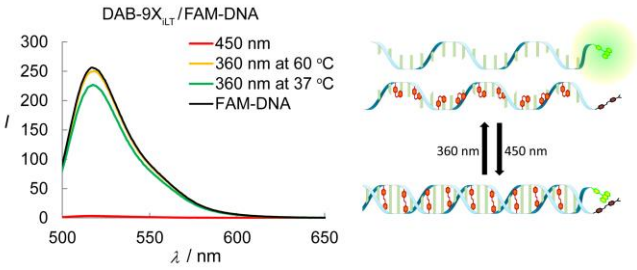

Figure 9. Fluorescence spectra of **DAB-9X$_{iLT}$/FAM-DNA** duplexes after irradiation with 450 nm (red line) and 360 nm light at 60 ^{o}C (yellow line) and at 37 ^{o}C (green line). Black line represents fluorescence from **FAM-DNA** single strand. Solution conditions were 100 nM **FAM-DNA**, 150 nM **DAB-9X$_{iLT}$**, 100 mM NaCl, 10 mM phosphate buffer (pH 7.0), ex. at 480 nm.

Conclusions

We synthesized the acyclic iL-threoninol scaffold to evaluate the effect of the position of methyl group on duplex stability by using *trans*-azobenzene as a typical planar functional molecule. All acyclic serinol derivatives efficiently stabilized DNA duplexes as long as the configuration of 2'-amino was fixed in a suitable orientation. The influence of the methyl group depended on the motif: First, in the wedge motif, azobenzene on the iL-threoninol scaffold stabilized the DNA duplex more efficiently than other scaffolds tested. Thus, we expect that the iL-threoninol scaffold will be useful in the context of linear probes containing multiple dyes.[15] Second, in dimer and cluster motifs, the D-threoninol scaffold resulted in a higher stability duplex than iL-threoninol and serinol scaffolds.[16] Finally, for applications that involve photo-regulation of hybridization with azobenzene-tethered DNA, the duplexes with *trans* and *cis* isomers of iL-threoninol had the largest differences in T_m of the scaffolds tested. In the context of the duplex evaluated, which contained nine azobenzenes, photo-regulatory efficiency did not significantly depend on the scaffold under physiological conditions. Based the analyses described, a suitable acyclic scaffold can be selected for use as a probe or in a nanomaterial application of DNA.

Experimental Section

Materials: Reagents and phosphoramidite monomers for DNA synthesis and Poly-Pak II cartridges were purchased from Glen Research. Other reagents for the synthesis of phosphoramidite monomers were purchased from Tokyo Kasei Co., Ltd., Wako Pure Chemical Industries, Ltd., and Aldrich. Unmodified DNA was purchased from Integrated DNA Technologies.

Synthesis and purification of oligonucleotides: All DNAs were synthesized using an ABI 3400 DNA/RNA synthesizer using phosphoramidite monomers containing azobenzene tethered to the described scaffolds. Synthesized oligonucleotides were purified using Poly-Pak cartridges and reversed-phase HPLC (Merck LiChrospher 100 RP-18(e) column). The **DAB-9X** oligonucleotides were purified by polyacrylamide gel electrophoresis followed by HPLC. Oligonucleotides were characterized by MALDI-TOF MS.

Results of MALDI-TOF MS: Oligonucleotides were characterized by MALDI-TOF MS (Autoflex II, BRUKER DALTONICS in positive mode). 3-Hydroxypyridine-2-carboxylic acid was used as a matrix. Spectra of all oligonucleotides are shown in supporting information. m/z calcd for **N-1X$_{iLT}$** [M+H$^+$]: 4020; found: 4020; m/z calcd for **N-1X$_S$** [M+H$^+$]: 4006; found: 4007; m/z calcd for **N-1X$_{DT}$** [M+H$^+$]: 4020; found: 4023; m/z calcd for **N-3X$_{iLT}$** [M+H$^+$]: 4770; found: 4773; m/z calcd for **N-3X$_S$** [M+H$^+$]: 4728; found: 4731; m/z calcd for **N-3X$_{DT}$** [M+H$^+$]: 4770; found: 4773; m/z calcd for **N-3X$_{iLT}$-c** [M+H$^+$]: 4770; found: 4772; m/z calcd for **N-3X$_S$-c** [M+H$^+$]: 4728; found: 4731; m/z calcd for **N-3X$_{DT}$-c** [M+H$^+$]: 4770; found: 4772; **C-1X$_{iLT}$** [M+H$^+$]: 4020; found: 4022; m/z calcd for **C-1X$_S$** [M+H$^+$]: 4006; found: 4008; m/z calcd for **C-1X$_{DT}$** [M+H$^+$]: 4020; found: 4021; m/z calcd for **C-3X$_{iLT}$** [M+H$^+$]: 4770; found: 4773; m/z calcd for **C-3X$_S$** [M+H$^+$]: 4728; found: 4732; m/z calcd for **C-3X$_{DT}$** [M+H$^+$]: 4770; found: 4774; m/z calcd for **C-3X$_{iLT}$-c** [M+H$^+$]: 4770; found: 4773; m/z calcd for **C-3X$_S$-c** [M+H$^+$]: 4728; found: 4731; m/z calcd for **C-3X$_{DT}$-c** [M+H$^+$]: 4770; found: 4773; m/z calcd for **FAM-DNA** [M+H$^+$]: 6617; found: 6618; m/z calcd for **DAB-9X$_{iLT}$** [M+H$^+$]: 9984; found: 9995; m/z calcd for **DAB-9X$_S$** [M+H$^+$]: 9858; found: 9870; m/z calcd for **DAB-9X$_{DT}$** [M+H$^+$]: 9984; found: 10002.

Melting-temperature measurements: Melting curves of DNA duplexes were obtained using a Shimadzu UV-1800 or a JASCO model V-560 spectrometer by measuring the change in absorbance at 260 nm versus temperature. The temperature ramp was 0.5 ^{o}C min^{-1} for the Shimadzu UV-1800 and 1.0 ^{o}C min^{-1} for the JASCO model V-560 spectrometer. The T_m was determined from the maximum in the first derivative of the melting curve. Both the heating and cooling curves were measured, and the obtained T_ms were within 2.0 ^{o}C. The solution conditions were 100 mm NaCl, 10 mm phosphate buffer (pH 7.0), 5.0 μM oligonucleotide. Melting curves of **DAB-9X/FAM-DNA** were obtained from the change of fluorescence intensity of FAM versus temperature by using a JASCO model FP-6500 spectrometer. Thermodynamic parameters were determined from $1/T_m$ versus ln (C_T/4) plots using the following equation: $1/T_m = R / \Delta H \ln (C_T/4) + \Delta S/\Delta H$, for which C_T is the total concentration of nucleic acid. $\Delta G°_{37}$ was calculated from the $\Delta H°$ and $\Delta S°$ values. The solution conditions were as follows: 100 mm NaCl, 10 mm phosphate buffer, pH 7.0. Concentrations were 0.25-4.0 μM for **DAB-9X/FAM-DNA** and 1.0-16.0 μM for other duplexes (Table S2).

CD measurements: CD spectra were measured using a JASCO model J-820 instrument equipped with a programmable temperature controller. The sample solutions contained 100 mm NaCl, 10 mm phosphate buffer (pH 7.0). The concentration of **DAB-9X/FAM-DNA** was 3.1 μM. The concentration of other oligonucleotides was 4.0 μM. Experiments were performed in a 10-mm quartz cell.

Computer simulation of structures of DNA duplex bearing azobenzene: MacroModel, version 10.4 (Schrödinger) was used for conformational energy minimization. First, a canonical B-form DNA duplex of the **N/C** sequence containing two extra base pairs at the centre was constructed. The extra base pairs were displaced with azobenzene and each scaffold. Before the energy minimization, conformational search around modified portion was briefly performed. The OPLS 2005 force field was used for the calculation.

Photoirradiation: A xenon light source (MAX-301, Asahi Spectra) equipped with interference filters centred at 360.0 nm (0.15 mW cm^{-2}) and 450.0 nm (half bandwidth 10-12 nm) were used for photoirradiation. The sample solution was added to a cuvette, and the temperature of light irradiation was controlled by using a programmable temperature controller. Photoirradiation of 450 nm light was conducted at 20 ^{o}C. Temperatures of 360 nm irradiation are described in main text.

Spectroscopic measurements: UV/Vis spectra were measured on a JASCO model V-560 spectrometer equipped with a programmable temperature controller; 10-mm quartz cells were used. Fluorescence spectra were measured on a JASCO model FP-6500 spectrometer equipped with a microcell holder.

Acknowledgements

This work was supported by the Scientific Research on Innovative Areas “Molecular Robotics” [no. 24104005], Grant-in-Aid for challenging Exploratory Research [no. 16K12522] from the Ministry of Education, Culture, Sports, Science and Technology, Japan. The support of the Asahi Glass Foundation (H.A.) is also acknowledged.

Keywords: DNA · oligonucleotides · Azo compounds · Photochromism · UV/Vis spectroscopy

[1] (a) E. T. Kool, *Acc. Chem. Res.* **2002**, *35*, 936-943; (b) A. A. Henry, F. E. Romesberg, *Curr. Opin. Chem. Biol.* **2003**, *7*, 727-733; (c) S. A. Benner, *Acc. Chem. Res.* **2004**, *37*, 784-797; (d) G. H. Clever, C. Kaul, T. Carell, *Angew. Chem*. **2007**, **119**, 6340–6350; *Angew. Chem. Int. Ed.* **2007**, *46*, 6226-6236; (e) P. Kočalka, N. K. Andersen, F. Jensen, P. Nielsen, *ChemBioChem* **2007**, *8*, 2106-2116; (f) A. T. Krueger, H. Lu, A. H. F. Lee, E. T. Kool, *Acc. Chem. Res.* **2007**, *40*, 141-150; (g) J. Štambaský, M. Hocek, P. Kočovský, *Chem. Rev.* **2009**, *109*, 6729-6764; (h) R. W. Sinkeldam, N. J. Greco, Y. Tor, *Chem. Rev.* **2010**, *110*, 2579-2619; (i) L. M. Wilhelmsson, *Q. Rev. Biophys.* **2010**, *43*, 159-183; (j) A. Okamoto, *Chem. Soc. Rev.* **2011**, *40*, 5815-5828; (k) I. Hirao, M. Kimoto, R. Yamashige, *Acc. Chem. Res.* **2012**, *45*, 2055-2065; (l) Y. Takezawa, M. Shionoya, *Acc. Chem. Res.* **2012**, *45*, 2066-2076; (m) K. Morihiro, O. Hasegawa, S. Mori, S. Tsunoda, S. Obika, *Org. Biomol. Chem.* **2015**, *13*, 5209-5214.

[2] (a) P. S. Miller, J. Yano, E. Yano, C. Carroll, K. Jayaraman, P. O. P. Ts'o, *Biochemistry (Mosc).* **1979**, *18*, 5134-5143; (b) M. H. Caruthers, *Acc. Chem. Res.* **1991**, *24*, 278-284; (c) Z. J. Lesnikowski, *Bioorg. Chem.* **1993**, *21*, 127-155; (d) P. E. Nielsen, *Annu. Rev. Biophys. Biomol. Struct.* **1995**, *24*, 167-183; (e) P. Herdewijn, *Liebigs Annalen* **1996**, *1996*, 1337-1348; (f) F. Eckstein, *Antisense Nucleic Acid Drug Dev.* **2000**, *10*, 117-121; (g) A. H. El-Sagheer, T. Brown, *Chem. Soc. Rev.* **2010**, *39*, 1388-1405; (h) N. Oka, T. Wada, *Chem. Soc. Rev.* **2011**, *40*, 5829-5843.

[3] (a) H. Inoue, Y. Hayase, A. Imura, S. Iwai, K. Miura, E. Ohtsuka, *Nucleic Acids Res.* **1987**, *15*, 6131-6148; (b) S. M. Freier, K.-H. Altmann, *Nucleic Acids Res.* **1997**, *25*, 4429-4443; (c) S. Obika, D. Nanbu, Y. Hari, J. Andoh, K. Morio, T. Doi, T. Imanishi, *Tetrahedron Lett.* **1998**, *39*, 5401-5404; (d) K. Yamana, R. Iwase, S. Furutani, H. Tsuchida, H. Zako, T. Yamaoka, A. Murakami, *Nucleic Acids Res.* **1999**, *27*, 2387-2392; (e) T. Wada, N. Minamimoto, Y. Inaki, Y. Inoue, *J. Am. Chem. Soc.* **2000**, *122*, 6900-6910; (f) C. J. Leumann, *Biorg. Med. Chem.* **2002**, *10*, 841-854; (g) M. Petersen, J. Wengel, *Trends Biotechnol.* **2003**, *21*, 74-81; (h) H. Saneyoshi, K. Seio, M. Sekine, *J. Org. Chem.* **2005**, *70*, 10453-10460; (i) Y. Doi, J. Chiba, T. Morikawa, M. Inouye, *J. Am. Chem. Soc.* **2008**, *130*, 8762-8768; (j) M. A. Campbell, J. Wengel, *Chem. Soc. Rev.* **2011**, *40*, 5680-5689.

[4] (a) T. Goldau, K. Murayama, C. Brieke, H. Asanuma, A. Heckel, *Chem. Eur. J.* **2015**, *21*, 17870-17876; (b) T. Goldau, K. Murayama, C. Brieke, S. Steinwand, P. Mondal, M. Biswas, I. Burghardt, J. Wachtveitl, H. Asanuma, A. Heckel, *Chem. Eur. J.* **2015**, *21*, 2845-2854.

[5] (a) U. B. Christensen, E. B. Pedersen, *Nucleic Acids Res.* **2002**, *30*, 4918-4925; (b) V. V. Filichev, E. B. Pedersen, *J. Am. Chem. Soc.* **2005**, *127*, 14849-14858; (c) B. Kou, X. Guo, S.-J. Xiao, X. Liang, *Small* **2013**, *9*, 3939-3943.

[6] (a) B. N. Trawick, T. A. Osiek, J. K. Bashkin, *Bioconjug. Chem.* **2001**, *12*, 900-905; (b) L. Bethge, I. Singh, O. Seitz, *Org. Biomol. Chem.* **2010**, *8*, 2439-2448; (c) S. S. Bag, S. Talukdar, R. Kundu, I. Saito, S. Jana, *Chem. Commun.* **2014**, *50*, 829-832.

[7] (a) R. Huber, N. Amann, H.-A. Wagenknecht, *J. Org. Chem.* **2004**, *69*, 744-751; (b) C. Wagner, H.-A. Wagenknecht, *Org. Lett.* **2006**, *8*, 4191-4194.

[8] H. Asanuma, H. Kashida, Y. Kamiya, *Chem. Rec.* **2014**, *14*, 1055-1069.

[9] H. Asanuma, T. Takarada, T. Yoshida, D. Tamaru, X. Liang, M. Komiyama, *Angew. Chem*. **2001**, *113*, 2743–2745; *Angew. Chem. Int. Ed.* **2001**, *40*, 2671-2673.

[10] H. Asanuma, T. Toda, K. Murayama, X. Liang, H. Kashida, *J. Am. Chem. Soc.* **2010**, *132*, 14702-14703.

[11] K. Murayama, H. Kashida, H. Asanuma, *Chem. Commun.* **2015**, *51*, 6500-6503.

[12] (a) H. Kashida, K. Murayama, T. Toda, H. Asanuma, *Angew. Chem*. **2011**, *123*, 1321–1324; *Angew. Chem. Int. Ed.* **2011**, *50*, 1285-1288; (b) K. Murayama, Y. Tanaka, T. Toda, H. Kashida, H. Asanuma, *Chem. Eur. J.* **2013**, *19*, 14151-14158.

[13] Y. Kamiya, H. Asanuma, *Acc. Chem. Res.* **2014**, *47*, 1663-1672.

[14] H. Asanuma, X. Liang, H. Nishioka, D. Matsunaga, M. Liu, M. Komiyama, *Nat. Protocols* **2007**, *2*, 203-212.

[15] H. Asanuma, M. Akahane, N. Kondo, T. Osawa, T. Kato, H. Kashida, *Chem. Sci.* **2012**, *3*, 3165-3169.

[16] Note that trans-azobenzene also has absorption at around 450 nm, although its absorption coefficient is smaller than that in *cis*-form

[17] H. Asanuma, T. Fujii, T. Kato, H. Kashida, *J. Photochem. Photobiol. C* **2012**, *13*, 124-135.

[18] J. L. Banks, H. S. Beard, Y. Cao, A. E. Cho, W. Damm, R. Farid, A. K. Felts, T. A. Halgren, D. T. Mainz, J. R. Maple, R. Murphy, D. M. Philipp, M. P. Repasky, L. Y. Zhang, B. J. Berne, R. A. Friesner, E. Gallicchio, R. M. Levy, *J. Comput. Chem.* **2005**, *26*, 1752-1780.

[19] H. Kashida, K. Sekiguchi, N. Higashiyama, T. Kato, H. Asanuma, *Org. Biomol. Chem.* **2011**, *9*, 8313-8320.

[20] Alternatively, the incomplete isomerization by multiple incorporation of azobenzene may also lose the priority of iL-threoninol scaffold. In other words, destabilization of *cis*-X_{iLT} might be cancelled by higher stabilization of *trans*-X_{iLT} which remained after UV-irradiation.

Entry for the Table of Contents (Please choose one layout)

Layout 1:

FULL PAPER

We synthesized an inverse L-threoninol (iL-threoninol) scaffold and compared its effect on DNA duplex stability to other acyclic artificial nucleic acid scaffolds that are based on D-threoninol and serinol. All three scaffolds stabilized DNA duplexes by intercalation of planar dye. The results indicated the properties of the iL-threoninol scaffold will make it a useful tether for dyes or other functionalities.

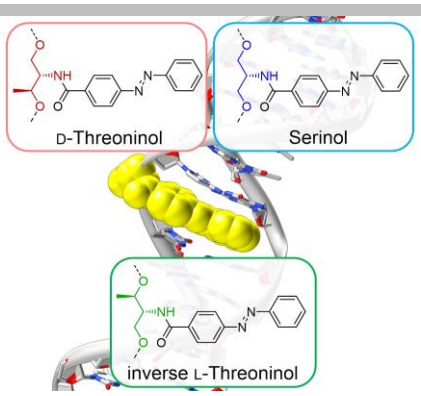

*Keiji Murayama, Hiroyuki Asanuma**

Page No. – Page No.

Effect of Methyl Group on Acyclic Serinol Scaffold for Tethering Dyes on DNA Duplex stability

Layout 2:

FULL PAPER

((Insert TOC Graphic here; max. width: 11.5 cm; max. height: 2.5 cm))

*Author(s), Corresponding Author(s)**

Page No. – Page No.

Title

Text for Table of Contents